INTERNATIONAL JOURNAL FOR NUMERICAL AND ANALYTICAL METHODS IN GEOMECHANICS, VOL. 20, 831–844 (1996)

A FINITE ELEMENT DOUBLE POROSITY MODEL FOR HETEROGENEOUS DEFORMABLE POROUS MEDIA

HAMID R. GHAFOURI* AND ROLAND W. LEWIS†

Civil Eng. Department, University of Wales, Swansea, SA2 888, U.K.

SUMMARY

The mathematical base of the double porosity concept, consisting of the continuity and equilibrium equation respectively, is briefly reviewed. A quasi-steady-state transfer function, the so-called *leakage term*, is used. Important aspects of the developed code, based on the double porosity theory, are presented together with two hypothetical example problems. The resulting trend of the settlements are compared to those from previous work and was found to be significantly different. However, the implications are that the present study exhibits a more realistic prediction for the settlement.

KEY WORDS: double porosity; consolidation; fissured material; coupled problems

1. INTRODUCTION

For many years, most of the effort for the simulation of fluid flow in fractured reservoirs had utilized average properties of the formation for both pores and fissures. Barrenblatt *et al.*[1] for the first time employed the concept of *double porosity* to present a model for simulating flow through rigid, fissured porous media. This work was followed by Warren and Root,[2] who presented an analytical solution for single-phase, unsteady-state flow in a naturally fractured reservoir. Subsequently, many studies have been carried out using the double porosity concept in which different properties have been attributed to the pores and fissures and this has proved to be a more reliable approach when dealing with a heterogeneous porous media. Most recently, the soil–fluid interaction caused by the soil deformation has also been included in the formulation to form coupled models which enables one to investigate the more realistic behaviour of fractured reservoirs, see for example, References 3–6 and 7–9. Although most of these studies have almost similar basic assumptions, they are different in their formulation and the solution procedure.

The model which will be presented throughout the paper is a new double porosity model where the basic assumptions are similar to those of previous works, but the formulation differs in several ways. Throughout the formulation, displacements, as well as pore pressures, are considered as primary unknowns and the final governing equations are fully coupled. Also, the well-established Finite Element Method has been used for solving the governing equations. This paper is in fact an introduction to the more complicated case of 3-phase, 3-dimensional fluid flow in a deformable heterogeneous porous media which would be presented in a later paper.

* Ph.D. student
† Professor

CCC 0363-906/96/110831-14

Received 7 September 1995
Revised 22 April 1996

2. DESCRIPTION OF THE MODEL

The basic mechanism of fluid flow in a fractured porous media may be explained as follows. The imposed external loads and/or well production both create a pressure gradient between the fluid within the matrix pores and the fluid in the adjacent fractures. The fluid within the matrix is squeezed out into the fissured continuum due to the produced gradient. Hence, flow towards the producing well takes place through the fissured network. In the present model, the fractured porous media is divided into two overlapping but distinct continuum, the first represents flow and deformation in the porous matrix while the second represents flow in the fissures (Figure 1). These two subdomains have the following characteristics:

1. The fluid flow within each subdomain is independent of the flow in the other subdomain and any coupling between the fluid flow in the porous matrix and the fissured network is controlled only by a *leakage* term, i.e. expelled fluid from the matrix which enters the fissures and *vice versa*. Hence, fluid pressure, saturation, porosity, permeability and the other properties of both the soil and fluids within the two subdomains are considered separately.
2. Within the first continuum the fluid flow is assumed to be coupled with the matrix deformation. This coupling is controlled via the rate of change of volumetric strain $\partial \varepsilon_{v1}/\partial t$.
3. It is assumed that the deformation of the first subdomain is only due to the total volumetric strain of the porous matrix and any change of volume of the solid particles is ignored.
4. Two different porosity values should be defined for the porous matrix and fissured region respectively, hence the term *double porosity model*, as follows:

$$\phi_1 = \frac{V_1}{V} \tag{1}$$

$$\phi_2 = \frac{V_2}{V} \tag{2}$$

where ϕ_1 and ϕ_2 are the porosity values of the porous matrix and fissured network respectively, V_1 and V_2 are the pore and fissured volume in a representative elementary volume (REV), and V is the total volume.

5. It is assumed that both the boundary and body forces are carried only by the porous matrix subdomain. Also, taking into account that the volume of the fractures is normally a small

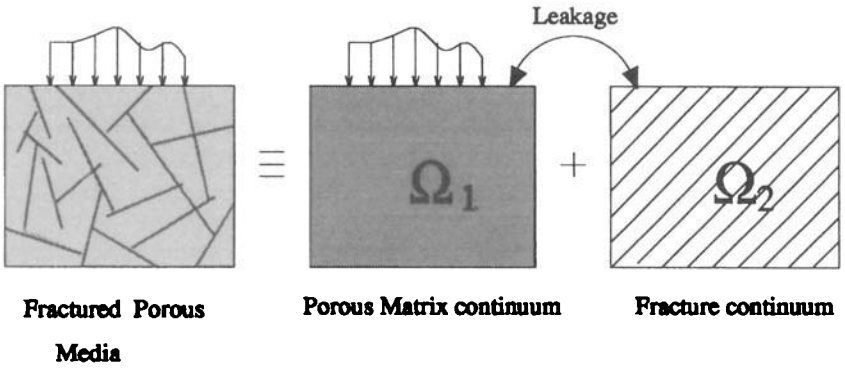

Figure 1. Schematic representation of double porosity model

fraction of the total void spaces, it is assumed that the compressibility of the fractured network does not alter the compressibility of the whole porous media dramatically and may be ignored.

6. Imbibition and depletion of fluid is via the fissured network subdomain only.
7. The two subdomains are assumed to be fully saturated.

3. DEVELOPMENT OF GOVERNING EQUATIONS

3.1. Equilibrium equation

Assuming that characteristic 5 is valid, the equilibrium equation for subdomain 1 would be obtained as follows. In a general form, the effective stress relationship is given by

$$\sigma_1 = (\sigma'_1 - m\bar{P}_1) \tag{3}$$

where σ_1 is the total stress, σ'_1 the effective stress, $\bar{P}_1$ the average fluid pressure within subdomain 1 and m is equal to unity for the normal stress components and zero for the shear stress components. In equation (3) the positive sign indicates tension. Also, the relationship between effective stress and strain can be written as follows:

$$\mathrm{d}\sigma'_1 = D_T(\mathrm{d}\varepsilon_1 - \mathrm{d}\varepsilon_0) + \mathrm{d}\sigma_0 \tag{4}$$

where D_T is the tangential stiffness matrix, which encompasses both elastic and plastic regions, ε_1 represents the strain of each medium caused only by the effective stress and ε_0 and σ_0 are the initial strain and initial stress values, respectively. Based on the principle of virtual work, the following equation can be written:

$$\left[\int_\Omega \delta\varepsilon^T\sigma\,\mathrm{d}\Omega - \int_\Omega \delta U^T b\,\mathrm{d}\Omega - \int_\Gamma \delta U^T\hat{t}\,\mathrm{d}\Gamma\right]_1 = 0 \tag{5}$$

where b and $\hat{t}$ are the body force and boundary tractions, respectively. An incremental form of the equilibrium equation can be written as

$$\left[\int_\Omega \delta\varepsilon^T\,\mathrm{d}\sigma\,\mathrm{d}\Omega - \int_\Omega \delta U^T\,\mathrm{d}b\,\mathrm{d}\Omega - \int_\Gamma \delta U^T\,\mathrm{d}\hat{t}\,\mathrm{d}\Gamma\right]_1 = 0 \tag{6}$$

Incorporating equation (3) into (6), the following expression is obtained:

$$\left[\int_\Omega \delta\varepsilon^T\,\mathrm{d}\sigma'\,\mathrm{d}\Omega - \int_\Omega \delta\varepsilon^T m\,\mathrm{d}\bar{P}\,\mathrm{d}\Omega + \mathrm{d}\hat{f}\right]_1 = 0 \tag{7}$$

where

$$\mathrm{d}\hat{f} = -\int_\Omega \delta U^T\,\mathrm{d}b\,\mathrm{d}\Omega - \int_\Gamma \delta U^T\,\mathrm{d}\hat{t}\,\mathrm{d}\Gamma + \int_\Omega \delta\varepsilon^T\,\mathrm{d}\sigma_0\,\mathrm{d}\Omega \tag{8}$$

represents the change in external force due to the boundary and body force loads. On substituting equation (4) into equation (7) and dividing $\mathrm{d}t$, the final form of the equilibrium equation results as follows:

$$\int_{\Omega_1} \delta\varepsilon_1^T D_T\frac{\partial\varepsilon_1}{\partial t}\,\mathrm{d}\Omega_1 - \int_{\Omega_1} \delta\varepsilon_1^T m\frac{\partial P_1}{\partial t}\,\mathrm{d}\Omega_1 + \frac{\partial\hat{f}}{\partial t} = 0 \tag{9}$$

3.2. Continuity equations

Let us consider a control volume V within a subdomain 1 and/or 2 which includes both pore and fissured voids. These two groups of voids can be denoted by ϕ_1 and ϕ_2, respectively. The continuity of fluid mass within this control volume can be written as follows:

$$\begin{pmatrix}\text{fluids inflow/outflow due}\\ \text{to pressure gradient within}\\ \text{each sub-domain}\end{pmatrix}+\begin{pmatrix}\text{fluids inflow/outflow due to}\\ \text{pressure gradient between}\\ \text{porous matrix and stiffness}\end{pmatrix}+\begin{pmatrix}\text{sink/source}\end{pmatrix}$$

$$+\begin{pmatrix}\text{rate of fluid accumulation}\\ \text{in the control volume}\end{pmatrix}=0$$

The various terms in the above equation will be discussed separately as follows.

1. Fluid inflow/outflow from the control volume due to a pressure gradient within each subdomain is given by

$$\nabla^{\mathrm{T}}\left[\rho_\alpha\left(\frac{-K_\alpha}{\mu}\nabla P_\alpha\right)\right] \tag{10}$$

2. Fluid inflow/outflow from control volume due to a pressure gradient between the porous matrix and the fissures, i.e. *leakage*, is

$$\pm\rho_1\frac{\bar{\alpha}K_1}{\mu}(P_1-P_2) \tag{11}$$

where $\bar{\alpha}$ is a coefficient which depends on the fissure width and geometry and could be determined as

$$\bar{\alpha}=\frac{4n(n+2)}{l^2} \tag{12}$$

where

$$l=\begin{cases} d_1 & \text{for } n=1 \quad (13)\\ \dfrac{2d_1d_2}{d_1+d_2} & \text{for } n=2 \quad (14)\\ \dfrac{3d_1d_2d_3}{d_1d_2+d_2d_3+d_1d_3} & \text{for } n=3 \quad (15)\end{cases}$$

where $n=1, 2, 3$ is the number of normal sets of fractures and d_1, d_2, d_3 are fracture intervals in each direction. For the sake of simplicity, the quasi-steady-state leakage term, as proposed by Barrenblatt *et al.*[1] and Warren and Root,[2] has been used throughout this paper. However, other forms of the transient leakage term[10,11] could be used in a similar manner.

3. Sink/source, which are assumed to be located within the fissured region only

$$\rho_0 Q \tag{16}$$

4. Rate of fluid accumulation in the control volume, obtained using the following expression:

$$\frac{\partial}{\partial t}(\rho_\alpha \phi_\alpha) = \phi_\alpha \frac{\partial \rho_\alpha}{\partial t} + \rho_\alpha \frac{\partial \phi_\alpha}{\partial t} \tag{17}$$

where
(a) the first term in the above relationship corresponds to the rate of fluid accumulation due to changes in density i.e.

$$\phi_\alpha \frac{\partial \rho_\alpha}{\partial t} \tag{18}$$

and
(b) the second term shows the rate of fluid accumulation due to a change of porosity, which in turn is influenced by three distinct factors
(i) the volumetric strain of each subdomain.
(ii) changes in particle due to fluid pore pressure.
(iii) changes in particle size due to effective stresses.
Usually, the latter two effects can be ignored because they are of less importance when compared to the former. Therefore, considering

$$\frac{\partial \phi_\alpha}{\partial t} = \frac{\partial \varepsilon_{v\alpha}}{\partial t} = m^{\mathrm{T}} \frac{\partial \varepsilon_\alpha}{\partial t} \tag{19}$$

where $m^{\mathrm{T}} = [1\ 1\ 1\ 0\ 0\ 0]$, the following expression may be written for the second term of equation (17), i.e.

$$\rho_\alpha m^{\mathrm{T}} \frac{\partial \varepsilon_\alpha}{\partial t} \tag{20}$$

On substituting equations (10), (11), (16), (17) and (19) into the continuity expression results in the following:

$$\nabla^{\mathrm{T}}\left(\frac{-\rho_\alpha K_\alpha}{\mu} \nabla P_\alpha\right) + (-1)^{\alpha+1} \rho_\alpha \frac{\bar{\alpha} K_1}{\mu}(P_1 - P_2) + (\alpha - 1)\rho_0 Q + \phi_\alpha \frac{\partial \rho_0}{\partial t} + (2 - \alpha)\rho_\alpha m^{\mathrm{T}} \frac{\partial \varepsilon_\alpha}{\partial t} = 0 \tag{21}$$

In fact, equation (21) exhibits two distinct relationships for $\alpha = 1, 2$ which correspond to the matrix and fissured region, respectively.

Equations (9) and (21) are the governing equations for the analysis of flow through a deformable fractured porous media where P_α and ε_α are the primary unknowns. Since all the non-linear coefficients are dependent on the unknowns, iterative procedures are performed within each time step to obtain the final solutions. For this purpose a fully implicit scheme should be applied.

4. FINITE ELEMENT DISCRETIZATION

A finite element method approach has been used throughout this study. If the primary unknowns P_α, U_1 at any point are approximated using shape functions e.g.

$$U_1 = N\bar{U}_1 \tag{22}$$

$$P_\alpha = \bar{N}\bar{P}_\alpha \tag{23}$$

where N, $\bar{N}$ are the shape functions and $\bar{U}_1$, $\bar{P}_\alpha$ are the nodal values for displacement and pressures, respectively, the following equilibrium equation would result:

$$\mathbf{K}_1 \frac{\mathrm{d}\bar{U}_1}{\mathrm{d}t} + \mathbf{L}_1 \frac{\mathrm{d}\bar{P}_1}{\mathrm{d}t} = \frac{\mathrm{d}\mathbf{f}_1}{\mathrm{d}t} \tag{24}$$

where

$$\mathbf{K}_1 = -\int_{\Omega_1} B^{\mathrm{T}} D_{T1} B \, \mathrm{d}\Omega_1 \tag{25}$$

$$\mathbf{L}_1 = -\int_{\Omega_1} B^{\mathrm{T}} m \bar{N} \, \mathrm{d}\Omega_1 \tag{26}$$

$$\mathrm{d}\mathbf{f}_1 = -\int_{\Omega_1} \bar{N}^{\mathrm{T}} \, \mathrm{d}b \, \mathrm{d}\Omega_1 - \int_{\Gamma_1} \bar{N}^{\mathrm{T}} \, \mathrm{d}\hat{t}_1 \, \mathrm{d}\Gamma_1 + \int_{\Omega_1} \mathrm{B}^{\mathrm{T}} \, \mathrm{d}\sigma_0 \, \mathrm{d}\Omega_1 \tag{27}$$

Having discretized equation (24) spatially, we must also consider the time domain as well. The time discretization method used is based on a Kantorovich[12] scheme. Basically, the time domain is divided into a number of elements, usually referred to as time steps, and then the integration is carried out to obtain the final solution of the unknowns. By assuming a linear variation of $\bar{U}_1$ and $\bar{P}_\alpha$ within each time step, as given by

$$N_1^t = 1 - \alpha_0 \tag{28}$$

$$N_2^t = \alpha_0 \tag{29}$$

where

$$\alpha_0 = \frac{t - t_k}{\Delta t_k} \tag{30}$$

the final form of the equilibrium equation used in the finite element approximation will be obtained as follows:

$$-(\mathbf{K}_1 \bar{U}_{1t_k} + \mathbf{L}_1 \bar{P}_{1t_k}) + (\mathbf{K}_1 \bar{U}_{1t_k+\Delta t_k} + \mathbf{L}_1 \bar{P}_{1t_k+\Delta t_k}) = \frac{\partial f}{\partial t} \Delta t_k \tag{31}$$

Similarly, the continuity equation for each continuum may be discretized spatially and temporally. As for all other boundary value problems, the governing differential equation for flow continuity, together with the appropriate boundary conditions, must be written in a weak form. This may be achieved by applying Green's theorem. On applying the same spatial shape function we have for the matrix continuum

$$\mathbf{H}_1 \bar{P}_1 + \mathbf{H}'(\bar{P}_1 - \bar{P}_2) + \mathbf{L}_1^{\mathrm{T}} \frac{\mathrm{d}\bar{U}_1}{\mathrm{d}t} + \mathbf{S}_1 \frac{\mathrm{d}\bar{P}_1}{\mathrm{d}t} = 0 \tag{32}$$

and for the fracture continuum,

$$\mathbf{H}_2 \bar{P}_2 - \mathbf{H}'(\bar{P}_1 - \bar{P}_2) + \mathbf{S}_2 \frac{\mathrm{d}\bar{P}_2}{\mathrm{d}t} = \bar{\mathbf{f}}_2 \tag{33}$$

where

$$\mathbf{H}_1 = \int_{\Omega_1} (\nabla \bar{N})^{\mathrm{T}} \frac{K_1}{\mu} \nabla \bar{N} \, \mathrm{d}\Omega_1 \tag{34}$$

$$\mathbf{H}_2 = \int_{\Omega_1} (\nabla \bar{N})^{\mathrm{T}} \frac{K_2}{\mu} \nabla \bar{N} \, \mathrm{d}\Omega_2 \tag{35}$$

$$\mathbf{H}' = \int_{1\&2} \bar{N}^{\mathrm{T}} \frac{\bar{\alpha} K_1}{\mu} \bar{N} \, \mathrm{d}\Omega_{1\&2} \tag{36}$$

$$\mathbf{S}_1 = \int_{\Omega_1} \bar{N}^{\mathrm{T}} \frac{\phi_1}{K_w} \bar{N} \, \mathrm{d}\Omega_1 \tag{37}$$

$$\mathbf{S}_2 = \int_{\Omega_2} \bar{N}^{\mathrm{T}} \frac{\phi_2}{K_w} \bar{N} \, \mathrm{d}\Omega_2 \tag{38}$$

$$\bar{\mathbf{f}}_2 = -\int_{\Gamma_2} \bar{N}^{\mathrm{T}} q_2 \, \mathrm{d}\Gamma_2 \tag{39}$$

Now, if we use the same temporal shape function as described previously, the next two continuity equations may be obtained.

For the matrix continuum:

$$\begin{aligned}[(1-\alpha_0)((\mathbf{H}_1+\mathbf{H}')\bar{P}_{1t_k} - \mathbf{H}'\bar{P}_{2t_k}) + \alpha_0((\mathbf{H}_1+\mathbf{H}')\bar{P}_{1t_k+\Delta t_k} - \mathbf{H}'\bar{P}_{2t_k+\Delta t_k})]\Delta t_k \\ + [-(\mathbf{L}_1^{\mathrm{T}}\bar{U}_{1t_k} + \mathbf{S}_1\bar{P}_{1t_k}) + (\mathbf{L}_1^{\mathrm{T}}\bar{U}_{1t_k+\Delta t_k} + \mathbf{S}_1\bar{P}_{1t_k+\Delta t_k})] = 0\end{aligned} \tag{40}$$

and for the fracture continuum:

$$\begin{aligned}[(1-\alpha_0)(-\mathbf{H}'\bar{P}_{1t_k} + (\mathbf{H}_2+\mathbf{H}')\bar{P}_{2t_k}) + \alpha_0(-\mathbf{H}'\bar{P}_{1t_k+\Delta t_k} + (\mathbf{H}_2+\mathbf{H}')\bar{P}_{2t_k+\Delta t_k})]\Delta t_k \\ + (-\mathbf{S}_2\bar{P}_{2t_k} + \mathbf{S}_2\bar{P}_{2t_k+\Delta t_k}) = \bar{\mathbf{f}}_2\Delta t_k\end{aligned} \tag{41}$$

Equations (31), (40) and (41) are the three governing equations which are shown in matrix form as follows

$$\begin{aligned}&\begin{bmatrix} \mathbf{K}_1 & \mathbf{L}_1 & 0 \\ \mathbf{L}_1^{\mathrm{T}} & \mathbf{S}_1 + \alpha_0(\mathbf{H}_1+\mathbf{H}')\Delta t_k & -\alpha_0\mathbf{H}'\Delta t_k \\ 0 & -\alpha_0\mathbf{H}'\Delta t_k & \mathbf{S}_2 + \alpha_0(\mathbf{H}_2+\mathbf{H})\Delta t_k \end{bmatrix} + \begin{bmatrix} \bar{\mathbf{U}}_1 \\ \bar{\mathbf{P}}_1 \\ \bar{\mathbf{P}}_2 \end{bmatrix}_{t_k+\Delta t_k} \\ &= \begin{bmatrix} \mathbf{K}_1 & \mathbf{L}_1 & 0 \\ \mathbf{L}_1^{\mathrm{T}} & \mathbf{S}_1 - (1-\alpha_0)(\mathbf{H}_1+\mathbf{H}')\Delta t_k & (1-\alpha_0)\mathbf{H}'\Delta t_k \\ 0 & (1-\alpha_0)\mathbf{H}'\Delta t_k & \mathbf{S}_2 - (1-\alpha_0)(\mathbf{H}_2+\mathbf{H})\Delta t_k \end{bmatrix} \begin{bmatrix} \bar{\mathbf{U}}_1 \\ \bar{\mathbf{P}}_1 \\ \bar{\mathbf{P}}_2 \end{bmatrix}_{t_k} + \begin{bmatrix} \frac{\mathrm{d}\bar{\mathbf{f}}_1}{\mathrm{d}t} \\ 0 \\ \bar{\mathbf{f}}_2 \end{bmatrix} \Delta t_k\end{aligned} \tag{42}$$

5. VALIDATION OF THE MODEL

The formulation presented in the foregoing sections was coded using the finite element method, with eight noded rectangular elements being used. In order to validate the developed code, it

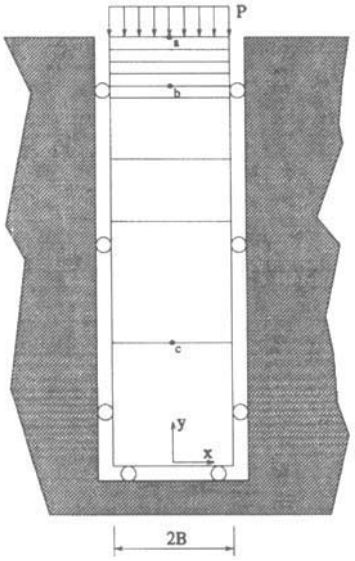

Figure 2. One-dimensional model problem and finite element mesh

would be advantageous to run examples of bench-mark problems. However, to the best knowledge of the authors there are no suitable problems available in the open literature, but a few hypothetical problems do exist in published works. Amongst these, two example problems given in References 12 and 13 were considered herein simply to illustrate the capabilities of the model. The former is a double porosity example where adequate initial data are given. The latter, also reported by Reference 14, is in fact a single porosity model which has the same general configuration of the former but with different material properties. The consequent results obtained by the assumption of a double porosity continuum were compared with the identical single porosity problem, and, as discussed later, the observed trend was deemed to be quite satisfactory.

The first problem as illustrated in Figure 2, is a one-dimensional column of soil subjected to a surface pressure P assuming plane strain conditions.

For the fractured continuum, the pore pressure was equal to zero at the top surface; everywhere else the surface of the body was assumed to be sealed and insulated. The matrix continuum, however, was assumed to be sealed at all boundaries due to assumption 6. The material properties and time step values used are indicated in Table I and II, respectively. The value α_0 used was 0·875.

The settlement values versus time are shown in Figure 3. The results obtained by the present study are significantly different from those of Reference 13. It may be observed that a more rapid surface settlement, as compared to the equivalent single porosity model, is predicted by the present study. This may be attributed to the presence of a fractured network within the porous body which results in a more rapid drainage of the fluid and consequently a faster rate of pore pressure dissipation. This behaviour, however, is reported in Reference 13 during the early time steps only and at later times the double porosity model exhibits a more sluggish response over the equivalent single porosity response.

Moreover, it may be observed that the final settlement predicted by this study is precisely the same value as that of the single porosity, while, unexpectedly, a lower value is predicted in

Table I. Example coefficients

Parameter (1)	Definition (2)	Magnitude Example 1 (3)	Magnitude Example 2 (4)	Units (5)
E	Modulus of elasticity	1.0	6×10^{-3}	MN/m^3
ν	Poisson's ratio	0.15	0.4	–
K_n	Fissure stiffness	0.1	–	$MN/m^2/m$
K_w	Fluid bulk modulus	0.1	∞	MN/m^2
ϕ_1	Matrix porosity	0.1	–	–
ϕ_2	Fissure porosity	0.05	–	–
k_1/μ	Matrix permeability	1×10^{-5}	4×10^{-6}	$m^4/(MNs)$
k_2/μ	Fissure permeability	1×10^{-1}	variable	$m^4/(MNs)$
d	Fissure spacing	0.025, 0.05, 0.1	0.1, 1.0, 1.5	m

Table II. Time steps for different time intervals – first example

Time interval (s)	Number of time steps
1.00E – 1	10
1.00E + 00	9
1.00E + 01	9
1.00E + 02	9
1.00E + 03	9
1.00E + 04	9
1.00E + 05	9
1.00E + 06	9
1.00E + 07	9
1.00E + 08	9
1.00E + 09	9
1.00E + 10	9

Reference 13. The fact that the fractured network facilitates the consolidation process makes it difficult to justify a lower value of settlement for the double porosity models. Therefore, the behaviour predicted by the present study seems to be more realistic. The unexpected results reported in Reference 13 make the following comment difficult to justify: "*The broad range of material parameters that influence the pressure generation and dissipation response makes meaningful representation of transient behavior difficult.*"†

The next problem is similar to the one available in References 13 and 14 but is for an isothermal case, as illustrated in Figure 2, where a unit surface load is applied to the column. Material properties are listed in Table I and the same initial and boundary conditions were assumed. The time step values used are indicated in Table III.

The code was run for the different K_1/K_2, ratios, i.e. the ratio of matrix permeability to fissured permeability. Also, different values were attributed to the fissure intervals, d, and the consequent

†Reference [7], page 118

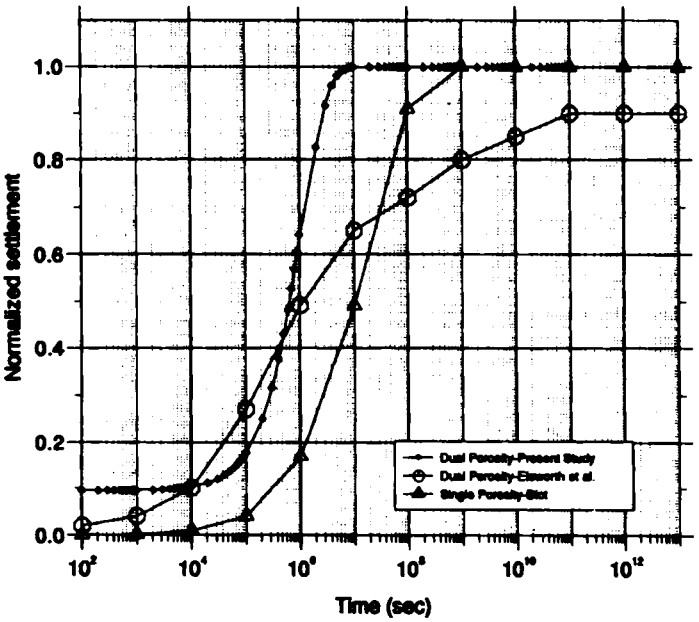

Figure 3. Surface displacement response for one-dimensional column loaded axially – example 1

Table III. Time steps for different time intervals – second example

Time interval (s)	Number of time steps
0.01	10
0.10	10
10	10
100	10
1000	20

results were compared. Figure 4 indicates the surface subsidence values for different K_1/K_2 ratios. As expected, the higher ratio will cause the more rapid consolidation. However, the final values of surface subsidence are the same for all cases, which again, is the expected result.

We would also expect to have a more rapid rate of consolidation for a highly fissured formation as compared to the ones with a lower degree of fissuring. This expectation agrees well with the result shown in Figure 5. In this case the values of permeability for both the matrix and fissured regions were considered constant and the only parameter changed during the different runs was the fracture interval.

The next observation deals with the variation of the pore pressure within the matrix and fracture continuum, respectively. One may predict that the pressure in the fractured network will decline faster than in the matrix continuum due to the higher permeability. This fact will cause the fluid within the fractures to be depleted rapidly. Figure 6 confirms this prediction, where the solid lines correspond to the matrix pore pressure and the dashed lines to the pore pressure values within the fractures.

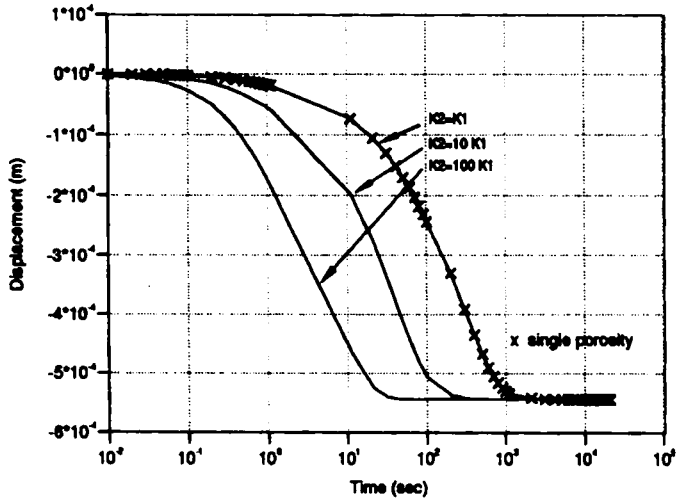

Figure 4. Surface subsidence for different fracture permeability

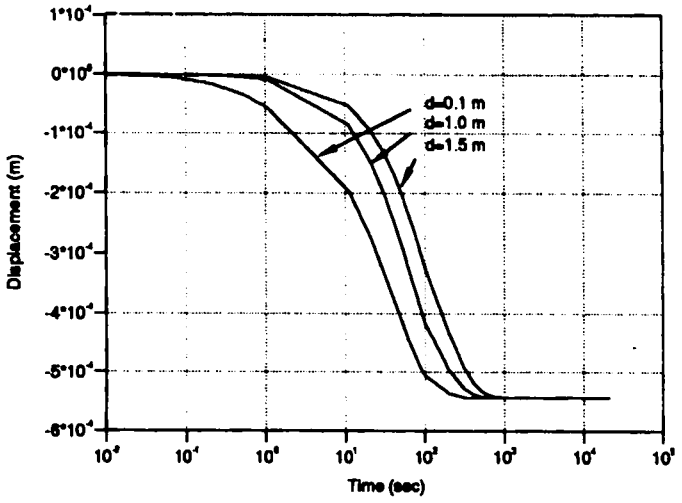

Figure 5. Surface subsidence for different fracture intervals

6. CONCLUSION

A finite element code, based on the theory of double porosity, has been presented. The hypothetical examples presented in the previous section may be considered as a proof of reliability of both the mathematical model and the developed code.

The results obtained by the present study are quite meaningful when compared to the equivalent single porosity model. However, the obtained trend is not similar to that of Reference 13. Hence, further numerical as well as experimental investigation of the behaviour is essential.

Also, as Figures 4, 5 and 6 suggest, the fractured porous media behaviour depends to a large extent on the fissure properties. Its behaviour is highly affected by both fissure permeability and

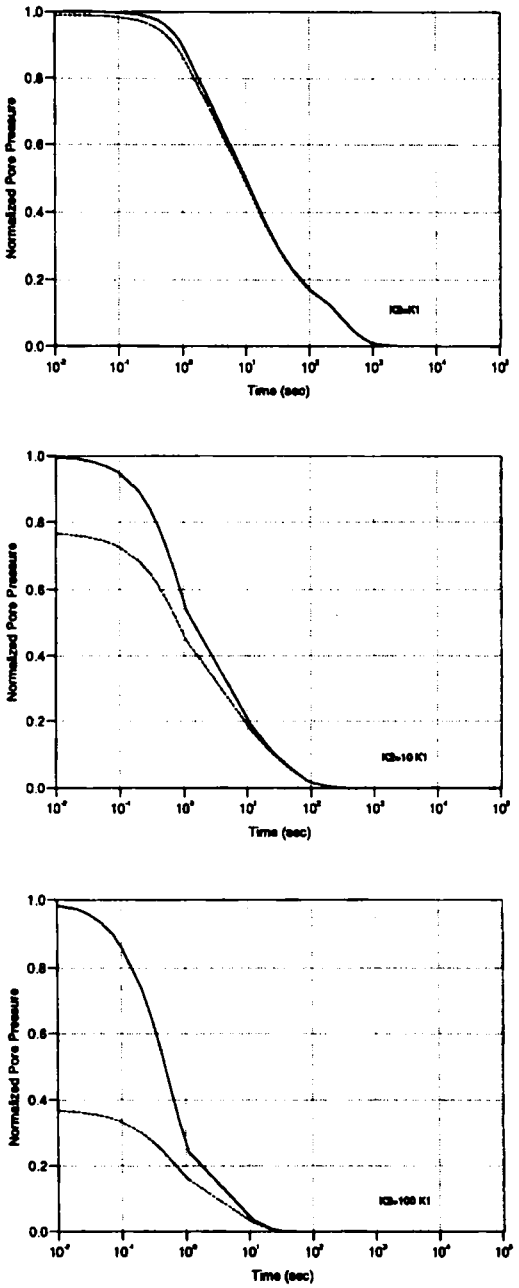

Figure 6. Matrix and fracture pore pressure at 'point b' for different K_1/K_2 ratios

fissure intervals. Therefore, a double porosity model is more realistic in such cases than those with a conventional single average porosity.

It should be noted that although a quasi-steady-state leakage term was used throughout the present study, this could easily be replaced by other transient forms.

Finally, the same concept and method could be applied in the case of three-dimensional, three-phase fluid flow (oil, gas and water) in fractured porous media, which is a case frequently encountered in petroleum reservoir simulation and will be the subject of a subsequent paper.

ACKNOWLEDGEMENT

One of the authors, H.R. Ghafouri, is grateful for the financial support given by the Ministry of Culture and Higher Education of the Islamic Republic of Iran.

APPENDIX: NOTATION

b	body force, FL^{-3}
d	fractures interval, L
E	module of elasticity, FL^{-2}
K	permeability, LT^{-1}
N	displacement shape function, –
$\bar{N}$	pressure shape function, –
N^t	time shape function, –
P	pore pressure, FL^{-2}
Q	inflow/outflow via sink/source, L^3T^{-1}
$\hat{t}$	boundary traction, FL^{-2}
V	fluid velocity, LT^{-1}

Greek letters

α_1	matrix porosity –
α_1	fracture porosity –
ε_v	volumetric strain –
$\bar{\alpha}$	fracture shape factor L^{-2}
α_0	time stepping factor –
μ	fluid viscosity FTL^{-2}
ρ	fluid density ML^{-3}
ρ_0	fluid density at a reference point ML^{-3}
σ_0	initial stress FL^{-2}
σ'	effective stress FL^{-2}
σ	total Stress FL^{-2}
ν	poisson ratio –

Super and subscripts

α	denoting matrix (1) and Fracture (2) continuum –
k	iteration level –
–	nodal values –
T	transported matrix –

REFERENCES

1. G. I. Barenblatt, I. P. Zheltov and I. N. Kochina, 'Basic concepts in the theory of seepage of homogeneous liquids in fissured rocks', *J. Appl. Math. Mech. USSR*, **24**, 1286–1303 (1960).
2. J. E. Warren and P. J. Root, 'The behavior of naturally Fractured Reservoirs', *SPE J. Trans. AIME*, **228**, 244–255 (1963).
3. E. C.Aifantis, 'Introducing a multi-porous medium', *Developments Mech.*, **9**, 46–69 (1985).
4. J. L. Auriault and C. Boutin, 'Deformable porous media with double porosity. Quasi-Statics. I: Coupling effects', *Trans. Porous Media*, **7**, 63–82 (1992).
5. M. Bai, Q. Ma and J. C. Roegiers, 'Dual-porosity behavior of naturally fractured reservoirs', *Int. j. numer. analyt. methods geomech.*, **18**, 359–376 (1994).
6. M. Bai, D. Elsworth and J. C. Roegiers, 'Modeling of naturally fractured reservoirs using deformation dependent flow mechanism', *Int. J. Rock Mech. Min. Sci. Geomech.*, **30**, 1185–1191 (1993).
7. H. Kazemi, 'Pressure transient analysis of naturally fractured reservoirs with uniform fracture distribution', *SPE J. Trans. AIME*, **246**, 451–461 (1969).
8. M. Y. Khaled, D. E. Beskos and E. C. Aifantis, 'On the theory of consolidation with double porosity', *Int. j. numer. analyt. methods geomech.*, **8**, 101–123 (1984).
9. M. Y. Khalili-Naghadeh, 'Numerical modelling of flow through fractured media', *Ph.D. Thesis*, Dept. Geotech. Eng., The University of NSW, Australia, 1991.
10. P. S. Huyakorn, B. H. Lester and C. R. Faust 'Finite element techniques for modeling ground water flow in fractured aquifers', *Water Resources Res.*, **19**, 1019–1035 (1983).
11. L.S.-K. Fung, 'Numerical simulation of naturally fractured reservoirs', *Proc. SPE Middle East Oil Technical Conference & Exhibition*, Bahrain, April 1993.
12. R. W. Lewis and B. A. Schrefler, *The Finite Element Method in the Deformation and Consolidation of Porous Media*, Wiley, New York, 1987.
13. D. Elsworth and M. Bai, 'Flow-deformation response of dual-porosity media', *J. geotech. eng. ASCE* **118**, 107–124 (1992).
14. B. L. Aboustit, S. H. Advani and J. K. Lee, 'Variational principles and finite element simulation for thermo-elastic consolidation', *Int. j. numer. analyt methods geomech.*, **9**, 49–69 (1985).